

# Neutron-irradiated superconducting $\text{YBa}_2\text{Cu}_3(\text{Li})\text{O}_{7-\delta}$ with improved irreversibility

V. SANDU\*, S. POPA, E. SANDU<sup>a</sup>, D. DI GIOACCHINO<sup>b</sup>, P. TRIPODI<sup>c</sup>

National Institute R&D of Materials Physics, Bucharest-Magurele, POBox MG-7, RO-077125, Romania

<sup>a</sup>National Institute of Physics and Nuclear Engineering "Horia Hulubei" Bucharest-Magurele, P.O. Box MG-6, RO-77125, Romania

<sup>b</sup>INFN-LNF, National Laboratory of Frascati, Via E. Fermi 40, 00044 Frascati, Italy

<sup>c</sup>Hydrogen Energy Research Agency, Corso della Repubblica 448, 00049 Velletri, Italy

Irradiation of  $\text{YBa}_2\text{Cu}_3(\text{Li})\text{O}_{7-\delta}$  ceramics with thermal and epithermal neutrons at fluences higher than  $10^{17}$  neutrons/cm<sup>2</sup> has led to a spectacular improvement of the intragranular properties. The critical current density has shown a monotonous dependence. The suppression of the critical temperature was below 2% but shows an increase at  $9.8 \times 10^{17}$  neutrons/cm<sup>2</sup>. This behaviour is consistent with the appearance of self-organized population of defects at high fluence. An analysis of the nature of the defect distribution, which is responsible for these effects, is provided.

(Received September 13, 2005; accepted January 26, 2006)

**Keywords:**  $\text{YBa}_2\text{Cu}_3$ , Neutron irradiation, Magnetization, *ac*-susceptibility, Critical current density

## 1. Introduction

The use of nuclear particle irradiation is an attractive option for the improvement of the pinning, hence of the capacity of current transport, in high temperature superconductors (HTS). The method looks interesting as long as the effects of the disorder associated with the irradiation have small or negligible effects on the rest of the important superconducting parameters. In the case of bulk samples, only neutrons seem to be efficient because of their large mean free path,  $\lambda \approx 1 \div 10$  cm, which permits a uniform distribution of the defects within sample.

Neutron-matter interaction is controlled by the neutron energy. At high particle energy, ( $E > 0.1$  MeV), neutrons remove the atomic species from their equilibrium position by direct knock on. The energy transfer of the neutron to the primary recoil atom is very high and produces a large spectrum of defects. The most affected are light or loosely bound atomic species, predominantly oxygen from  $\text{CuO}_x$  chains.

Thermal neutrons ( $E < 0.1$  MeV) interact in a more complex way: first the nucleus captures the neutron becoming unstable and fissions into high energetic products. The products released subsequent the fission remove and transmit energy to the crystal constituents which further collide and remove other atomic species. The process stops when all moving particles reach the thermal equilibrium in interstitial position. The result is the generation of vacancy-interstitial (Frenkel) defects that, owing to the thermal energy of the lattice, either annihilate by recombination or diffuse fast toward sinks. Depending on the specific absorption bias and strength of

each sink, the interstitials or vacancies might either accumulate near these pre-irradiative defects or be thermally released back to the bulk. Finally, it results cascades of less mobile vacancy and interstitial loops, which shrink or expand by point defect absorption or release. The anisotropy of the crystal structure has a strong influence on the defect distribution and, in certain cases, leads to a self-organization of nano- and microdefects.

In the case of HTS, the use of thermal neutrons has a drawback arising from the small effective cross section  $\sigma$  of the atomic constituents for the neutron capture. This disadvantage can be overwhelmed by inserting high  $\sigma$  atoms within superconducting matrix [1]. The main requirement is the absence of any deleterious effect on superconductivity of the inserted atoms. The best candidates are lithium [2-5] and uranium [6-8], which display important cross section and match well with HTS materials. Our investigation on LiF - doped  $\text{YBa}_2\text{Cu}_3\text{O}_{7-x}$  (YBCO-LiF) proved that this material maintains rather high critical temperatures up to 10 at % Li and keeps an unmodified orthorhombic structure up to 15 at % Li [9].

The effect of irradiation on the superconducting properties is not always monotonic but strongly biased by the nature and amount of the pre-irradiative defects. Therefore, even though most papers report a *degradation* of the critical temperature  $T_c$  and an *enhancement* of the critical current density  $J_c$  subsequent irradiation, there are also reports claiming an *enhancement* of the critical temperature for fluences around  $10^{16}$  cm<sup>-2</sup> associated with a *J<sub>c</sub> drop off* [10,11]. The effect was attributed to the prevalence of radiation stimulated recombination rate of the pre-irradiative defects over the defect generation [12].

In this paper we report the effect of  $T_c$  recovering at high fluences,  $\Phi > 5 \times 10^{17} \text{ cm}^{-2}$ , coupled with an increase of the intragranular critical current densities and the enhancement of the intragranular response in agreement with the irradiation triggered self-organization of the damages.

## 2. Experimental

Samples with the formal stoichiometry  $\text{YBa}_2\text{Cu}_3\text{O}_{7-x}$ , containing 2 at % lithium fluoride as additives were prepared by standard ceramic route. High purity  $\text{Y}_2\text{O}_3$ ,  $\text{BaCO}_3$ ,  $\text{CuO}$ , and  $\text{LiF}$  powders were calcined in flowing oxygen at  $930^\circ\text{C}$  for 20 hours. The product was reground, pressed in bar shapes of  $2.7 \times 2.9 \times 9 \text{ mm}^3$ , and sintered in flowing oxygen for 16 hours at  $936^\circ\text{C}$ . X-ray diffraction patterns samples reveal the pure orthorhombic phase but small amounts of  $\text{BaCuO}_2$ , are also present.

The dependence of the electric resistance on temperature was measured by four point method as the average value for two opposite current flows and for different values of the measuring current. The critical temperature was of  $93.6 \text{ K}$ .

Sample irradiation was performed inside the reactor VVRS from IFIN-”HH”-Magurele, channel 36/6, a dry channel with a flux density of  $2.13 \times 10^{13} \text{ cm}^{-2} \cdot \text{s}^{-1}$ , allowing a direct transfer of the samples inside the hot chambers. The neutronic characteristics of this channel were determined by absolute measurements and shows that more than 87 % of the neutrons have the energy below 1 MeV [13]. The samples, sealed within quartz ampoules, were irradiated in standard aluminium blocks suspended in the centre of the channel by means of a nylon thread. The used fluences were in a range between  $0.98 \times 10^{17}$  and  $9.98 \times 10^{17} \text{ cm}^{-2}$ . After irradiation, the samples were stored in the hot chamber for 7 days. During the irradiation, the sample temperature was not measured, but the channel temperature was below  $40^\circ\text{C}$ .

The magnetization dependence of the irradiated samples on the applied magnetic field at low magnetic fields (0-150 kA/m) and  $77 \text{ K}$  was carried out with an integrating magnetometer (Thor Cryogenics model 9020 II).

The  $ac$ -susceptibility, including the higher harmonics, were measured with a home made susceptometer with an  $ac$  driving magnetic field had an amplitude of  $0.6 \text{ mT}$  at a frequency of  $f = 1070 \text{ Hz}$ . The sample was mounted on a sapphire holder inserted in one of the pick up coils. The temperature was measured with a platinum thermometer (PT100) in thermal contact with the samples. The measurements were performed on sweeping the temperature at a rate of  $0.3 \text{ K/min}$  up to a temperature greater than the zero field critical temperature of the samples, i.e., between  $70 \text{ K}$  and  $110 \text{ K}$ . The induced signal has been measured with a multi-harmonic EG&G lock-in amplifier. The  $ac$  field was applied parallel to longest size of the sample.

## 3. Results and discussion

Fig. 1 shows the evolution of the magnetization at low magnetic field under neutron irradiation. On the basis of magnetization loops, the intragranular critical current density,  $J_c$ , was obtained using the Bean relationship

$$J_c = \frac{3(M^+ - M^-)}{D}$$

Here  $M^+(M^-)$  is the descending (ascending) branch of the hysteresis loop and  $D$  is the average grain size. It is clear that the irreversibility  $\Delta M = M^+ - M^-$ , hence, the critical current density, increases monotonically with the increase of the neutron fluence (Fig. 2). Additionally, the loop asymmetry relative to zero magnetization line decreases, as can be seen from the evolution of the equilibrium magnetization

$$M_{eq} = \frac{M^+ + M^-}{2} \quad (\text{see the Inset to Fig. 2}).$$

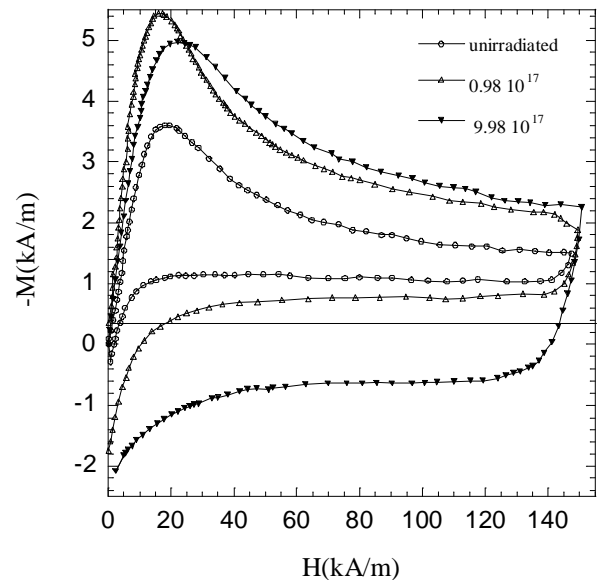


Fig. 1. Magnetization  $M$  vs applied magnetic field  $H$  at  $77 \text{ K}$  for polycrystalline Li-doped  $\text{YBa}_2\text{Cu}_3\text{O}_{7-x}$  submitted to neutron irradiation at the following fluences 0;  $0.98 \times 10^{17}$  and  $9.98 \times 10^{17} \text{ cm}^{-2}$ .

The increase of the pinning is expected after irradiation and is due to the increase of the defect density. As about the decrease of  $M_{eq}$ , it is due to the changes in the grain surface characteristics. It is accepted that the asymmetry is due to the surface pinning [14] which is reduced by the accumulation of the defects at the grain surface [15]. However, the critical temperature, as obtained from resistance vs temperature measurements is non-monotonic. First, it shows a continuous decrease with increasing the fluence up to  $4.9 \times 10^{17} \text{ cm}^{-2}$ , but displays an unexpected increase at the highest fluence (Fig. 3).

The complexity of the processes is revealed by the evolution of the  $ac$ -susceptibility, fundamental and higher harmonics.

The imaginary part of the fundamental harmonic  $\chi''$ , which reflects the loss of energy during one  $ac$ -cycle,

shows a reduction and a shift of the *intergranular* peak (seen at 84 K in the unirradiated sample). The shoulder seen at higher temperature  $\chi_p$  (marked with arrow in Fig. 4), which is attributed to the *intragranular* response (the temperature at which the Abrikosov vortices penetrate the grain and reach its centre), is shifted with only 0.7 K at  $0.98 \times 10^{17} \text{ cm}^{-2}$ . It transforms in a well defined peak, less shifted at  $9.8 \times 10^{17} \text{ cm}^{-2}$ .

The absolute value of the fundamental harmonics diminishes its amplitude, hence, the diamagnetic screening with increasing the fluence, but displays a higher uniformity at highest fluence (see the Inset to Fig. 4).

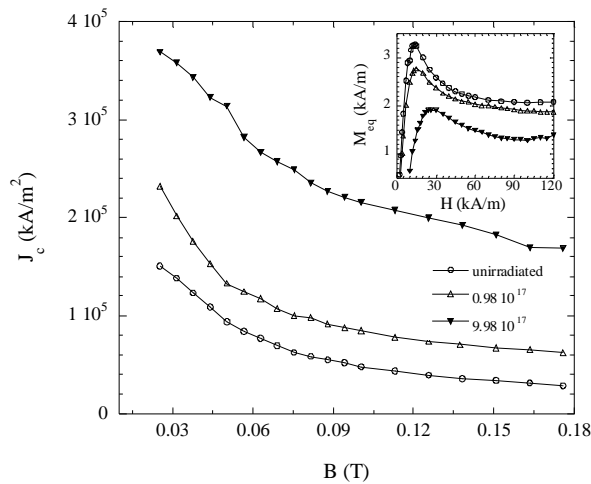


Fig. 2. Intragranular critical current density  $J_c$  at 77 K of polycrystalline Li-doped  $\text{YBa}_2\text{Cu}_3\text{O}_{7-x}$  submitted to neutron irradiation at the following fluences 0;  $0.98 \times 10^{17}$  and  $9.98 \times 10^{17} \text{ cm}^{-2}$ . Inset: the equilibrium magnetization for the same samples.

The higher harmonics,  $\chi_2$  (Fig. 5(a)) and  $\chi_3$  (Fig. 5 (b)), show more dramatic changes. The second harmonic, which in Bean model is supposed to be zero, has the amplitude of the same order with the third harmonic. It displays a complex structure for the virgin sample that is caused by those effects which produce the asymmetry of the hysteresis loop (surface barriers, trapped fields, etc). At the highest fluence,  $9.8 \times 10^{17} \text{ cm}^{-2}$ , the amplitude of the  $\chi_2$  is reduced and the small, positive peak at 90 K, which we attribute to the intragrain contribution, is no more visible. Meanwhile, the real part  $\chi_2'$  loses its structure. These facts confirm the assumption that the surface barriers are spoiled by irradiation.

The third harmonic  $\chi_3$  also displays reduced values after irradiation (Fig. 6). The small peak near the irreversibility temperature at 90 K shifts with 2 K downward but, surprisingly, it becomes more emphasized at  $9.98 \times 10^{17} \text{ cm}^{-2}$ . The large, negative peak at 86.6 K, which we attribute to the intergranular response, is broadened and shifted below 70 K.

A common characteristic of all harmonics is the rapid reduction of the intergranular peak and its shift with more than 10 K, whereas the extremes reflecting the

intragranular response are less shifted and their amplitude enhanced.

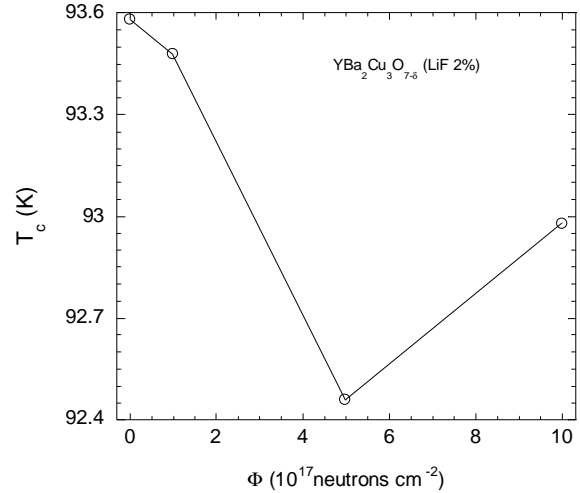


Fig. 3. The dependence of the critical temperature  $T_c$  of irradiated polycrystalline Li-doped  $\text{YBa}_2\text{Cu}_3\text{O}_{7-x}$  on the neutron fluence  $\Phi$ .

The different evolution of the inter- and intragranular characteristics under irradiation field advocates for the alteration of the homogeneous distribution of the built up defects which is seen at fluences of order of  $10^{17} \text{ cm}^{-2}$  and its transformation, at high irradiation time, in a spatially non-uniform one despite a homogeneous generation by irradiations. Specifically, at the highest fluence, the damages accumulate mainly in the intergrain areas and the grains become cleaner. This fact contrasts with the almost uniform degradation of the superconductivity as observed in susceptibility experiments up to  $0.98 \times 10^{17} \text{ cm}^{-2}$  and up to  $4.9 \times 10^{17} \text{ cm}^{-2}$  in resistance measurements.

Theoretically, the spatial distribution of damages and their evolution under irradiation were examined in the framework of the irradiation induced self-organization of the defects [17] controlled by diffusional reactions. The nonlinear equation describing the complex process of generation, diffusion, and annihilation of the defects possesses a bifurcation point which could lead to self-organization of the defect distribution [18]. The self-organization of defects, including pattern formation, occurs when, besides the mobile defects, vacancies and interstitials, less mobile clusters of vacancies are also produced, due to the higher value of the diffusion constant of interstitials relative to vacancies.

The clusters of vacancies are kind of sink with a biased capture efficiency different from other sinks (pre-irradiative defects) [17]. These are the minimal conditions required to develop instabilities in the solution of the nonlinear diffusion-reaction equation describing the damage production by irradiations [17,19,20]. At high enough fluence, the spatially homogeneous vacancy loop population develops spatial instabilities if the dislocation bias overcomes the cascade-collapse efficiency  $\varepsilon = 1 - \kappa_v/\kappa_i$ , where  $\kappa_i$  ( $\kappa_v$ ) is the rate of interstitials (vacancies) production. The result is a sharp defect

distribution around sinks, and a reduction of their density faraway from these sinks. In strongly anisotropic systems, a pattern consisting of a regular system of parallel stripes of defects alternating with “clean” material [21] was obtained by computer simulations.

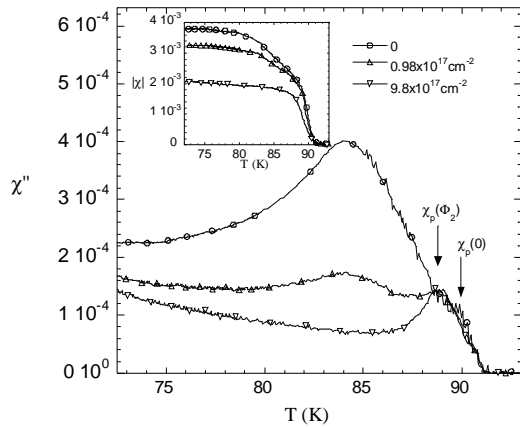


Fig. 4. The imaginary component  $\chi''$  of the fundamental harmonic of the ac-susceptibility of polycrystalline Li-doped  $\text{YBa}_2\text{Cu}_3\text{O}_{7-x}$  as a function of temperature  $T$  submitted to neutron irradiation at following fluences 0;  $0.98 \times 10^{17}$  and  $9.98 \times 10^{17} \text{ cm}^{-2}$ . Inset: the modulus of the ac-susceptibility  $|\chi|$  for the same samples.

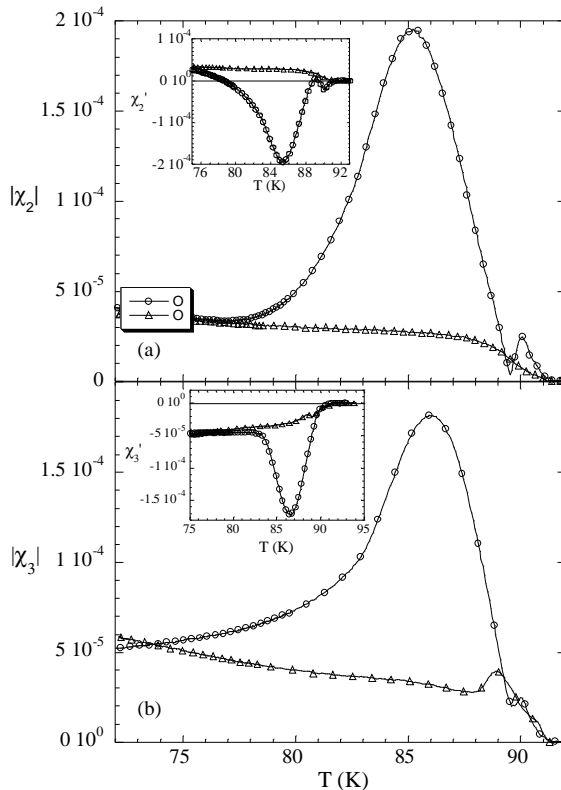


Fig. 5. The dependence of the  $|\chi_2|$  (a) and  $|\chi_3|$  of ac-susceptibility on temperature  $T$  of polycrystalline Li-doped  $\text{YBa}_2\text{Cu}_3\text{O}_{7-x}$  before irradiation (circles) and after neutron irradiation at  $9.98 \times 10^{17} \text{ cm}^{-2}$  (triangles). Insets: the real components  $\chi'_2$  and  $\chi'_3$  for the same sample.

This picture explains the dependence of both resistance and susceptibility observed at highest fluence if we consider that the grain border is the sink with the highest strength and poses a large bias factor. At the border, the density of pre-irradiative defects is extremely high and consists mainly of disorder in the oxygen sublattice [22,23].

At low fluence,  $0.98 \times 10^{17} \text{ cm}^{-2}$ , the defect distribution is almost uniform within each grain and corresponds to the homogeneous solution of the reaction-diffusion equations. The vacancy clusters do not display the value required by the bifurcation condition. Therefore, the increase of the density of homogeneously distributed of defects depresses the superconducting order parameter, hence, decreases the intragranular peak, and the diamagnetic screening. However, this fact increases the intragranular critical current density.

The point defects, which are absorbed by the border sinks, contribute to the increase of the effective thickness of the intergrain Josephson junction. Subsequently, the intergranular critical current density  $j_c$  is fast suppressed because of its exponential decrease with the enlargement of the barrier thickness.

The reduction of the second harmonic at the highest fluence and the fading of the intragranular peak corroborates with the accretion of defects, hence, pinning centres, at the grain border. These surface pinning centres suppress the surface (Bean-Livingstone) barriers, which require a clean grain surface, and are responsible for both the increased asymmetry of hysteresis loops and the height of the first magnetization peak.

The spectacular recovery and the enhancement of the intragranular superconducting properties at the highest fluence  $\Phi_2 = 9.98 \times 10^{17} \text{ cm}^{-2}$  reflect the effect of the self-organization of defects, which creates a sharp distribution of defect concentration in the sink areas, but also clean, defectless superconducting regions. When the clean areas have a size much larger than the in-plane coherence length, they can be regarded as good superconducting regions which can reach more or less the grain size. This explains the raise of the critical temperature (Fig. 3) as well as the enhancement of the intragranular response displayed by the fundamental (Fig. 4) and the third harmonics (Fig. 5b) at the highest fluence. On the other hand, those regions with high defect population and abrupt profile of the space variation of the defect distribution function are able to create an abrupt profile of field inside the grains, hence, a high critical current densities ( $J_c = \nabla \times H$ ).

In conclusion, we have evidenced for the first time that ceramic superconductors submitted to neutron irradiation display responses which agree with the development of self-organized distribution of damages.

## Acknowledgements

The research was supported in part by the European Community under the TARI contract HPRI-CT-1999-00088 and by Romanian Ministry of Education and

Science in the framework of the MATNANTECH project 260/2004.

### References

- [1] R. L. Fleischer, H. R. Hart Jr., K.W. Lay, F. E. Luborsky, *Phys. Rev. B* **40**, 2163 (1989).
- [2] M. Eisterer, S. Tönies, W. Novak, H. W. Weber, R. Weinstein, R. Sawh, *Supercond. Sci. Technol.* **11**, 1001 (1998).
- [3] V. Sandu, S. Popa, J. Jaklovszky, E. Cimpoiasu, *J. Supercond.* **11**, 251 (1998)
- [4] F. Vasiliu, V. Sandu, P. Nita, S. Popa, E. Cimpoiasu, M. C. Bunesco, *Physica C* **303**, 209 (1998).
- [5] M. Turchinskaya, D. L. Kaiser, A. J. Shapiro, J. Schwartz, *Physica C* **246**, 34 (1995).
- [6] R. Weinstein, Y. Ren, J. Liu, I. G. Chen, R. Sawh, C. Foster, V. Obot, *Proc. Int. Symp. on Superconductivity*, (Hiroshima, 1993), (Tokyo: Springer), p. 855, 1994.
- [7] Y. Ren, R. Weinstein, R. Sawh, *Physica C* **282**, 2275 (1997).
- [8] R. Weinstein, R. Sawh, Y. Ren, M. Eisterer, H. W. Weber, *Supercond. Sci. Technol.* **11**, 959 (1998).
- [9] V. Sandu, J. Jaklovszky, Gh. Aldica, E. Cimpoiasu, M. C. Bunesco, *Balkan. Phys. Lett.* **6**, 238 (1998).
- [10] R. F. Konopleva, B. L. Oksengendler, A. K. Pustovoi, B. Borisov, V. A. Chekanov, M. V. Chudakov, *Sverkh. Fiz. Him. Tekh.* **3**, 568 (1993).
- [11] V. Sandu, S. Popa, J. Jaklovszky, E. Cimpoiasu, *J. Supercond.* **11**, 251 (1998).
- [12] V. Sandu, *Rom. J. Phys* **45**, 487 (2000).
- [13] C. Miron, C. Garlea, I. Garlea, V. Raducu, *Rev. Roum. Phys.* **31** (1968) 813.
- [14] M. Konczykowski, L. Burlachkov, Y. Yeshurun, F. Holtzberg, *Phys. Rev. B* **43**, 13707 (1991).
- [15] A. E. Koshelev, V. M. Vinokur, *Phys. Rev B* **64**, 134518 (2001).
- [16] K. Krishan, *Nature (London)* **287**, 420 (1980).
- [17] H. Trinkhaus, C. Abromeit, J. Villain, *Phys. Rev. B* **40**, 12531 (1989).
- [18] G. Nicolis, I. Prigogine, *Self-Organization in Non-Equilibrium Systems*, Wiley, New York, 1977.
- [19] D. Walgraef, N. M. Ghoniem, *Phys. Rev. B* **39**, 8867 (1989); **52**, 3951 (1995).
- [20] D. Walgraef, J. Lauzeral, N. M. Ghoniem, *Phys. Rev. B* **53**, 14782 (1996).
- [21] N. M. Ghoniem, D. Walgraef, S. J. Zinkle, *J. Computer. Aid. Mater. Design* **8**, 1 (2002).
- [22] B. H. Moeckly, D. K. Lathrop, R. A. Buhrman, *Phys. Rev. B* **47**, 400 (1993).
- [23] C. Betouras, R. Joynt, *Physica C* **250**, 256 (1995).

\* Corresponding author: vsandu@infim.ro